



This is a repository copy of *A 3-parameter analytical model for the acoustical properties of porous media*.

White Rose Research Online URL for this paper:
<http://eprints.whiterose.ac.uk/144499/>

Version: Accepted Version

Article:

Horoshenkov, K. orcid.org/0000-0002-6188-0369, Hurrell, A. and Groby, J.-P. (2019) A 3-parameter analytical model for the acoustical properties of porous media. *The Journal of the Acoustical Society of America*, 145 (4). pp. 2512-2517. ISSN 0001-4966

<https://doi.org/10.1121/1.5098778>

Copyright 2019 Acoustical Society of America. This article may be downloaded for personal use only. Any other use requires prior permission of the author and the Acoustical Society of America. The following article appeared in *The Journal of the Acoustical Society of America* 2019 145:4, 2512-2517 and may be found at <https://doi.org/10.1121/1.5098778>

Reuse

Items deposited in White Rose Research Online are protected by copyright, with all rights reserved unless indicated otherwise. They may be downloaded and/or printed for private study, or other acts as permitted by national copyright laws. The publisher or other rights holders may allow further reproduction and re-use of the full text version. This is indicated by the licence information on the White Rose Research Online record for the item.

Takedown

If you consider content in White Rose Research Online to be in breach of UK law, please notify us by emailing eprints@whiterose.ac.uk including the URL of the record and the reason for the withdrawal request.



eprints@whiterose.ac.uk
<https://eprints.whiterose.ac.uk/>

1 A 3-parameter analytical model for the acoustical properties of porous media

2 Kirill V. Horoshenkov,¹ Alistair Hurrell,¹ and Jean-Philippe Groby²

3 ¹*Department of Mechanical Engineering, University of Sheffield, Sheffield, S1 3JD,*
4 *UK^a*

5 ²*Laboratoire d'Acoustique de l'Universit du Mans, LAUM - UMR CNRS 6613,*
6 *Le Mans Universit, Avenue Olivier Messiaen, 72085 LE MANS CEDEX 9,*
7 *France*

8 Many models for the prediction of the acoustical properties of porous media require
9 non-acoustical parameters few of which are directly measurable. One popular predic-
10 tion model by Johnson, Champoux, Allard and Lafarge [Champoux *et al*, J. Appl.
11 Phys, 70(4), 1975 – 1979 (1991)] (334 citations, Scopus, December 2018) requires
12 six non-acoustical parameters. This paper proves that the use of more than three
13 parameters in the Johnson-Champoux-Allard-Lafarge model is not necessary at all.
14 Here we present theoretical and experimental evidence that the acoustical impedance
15 of a range of porous media with pore size distribution close to log-normal (granular,
16 fibrous and foams) can be predicted through the knowledge of the porosity, median
17 pore size and standard deviation in the pore size only. A novelty of this paper is
18 that it effectively halves the number of parameters required to predict the acoustical
19 properties of porous media very accurately. The significance of this paper is that
20 it proposes an unambiguous relationship between the pore microstructure and key
21 acoustical properties of porous media with log-normal pore size distribution. This
22 new model is well suited for using acoustical data for measuring and inverting key
23 non-acoustical properties of a wider range of porous media used in a range of appli-
24 cations which are not necessarily acoustic.

^{a)}k.horoshenkov@sheffield.ac.uk

A 3-parameter analytical model for the acoustical properties of porous media

²⁵ PACS: 43.20 Mv, 43.20 Ye, 43.55 Ev, 43.58 Bh

²⁶ Keywords: Porous media, acoustic impedance, sound propagation

27 **I. INTRODUCTION**

28 The model for the acoustical properties of porous media proposed by Champoux, Allard
 29 and Lafarge^{1,2} relies on six non-acoustical parameters which are: (i) porosity (ϕ), (ii) tor-
 30 tuosity (α_∞); (iii) viscous characteristic length (Λ); (iv) thermal characteristic length (Λ');
 31 (v) viscous permeability (κ_0); and (vi) thermal permeability (κ'_0). The improved model pro-
 32 posed by Pride³ adds one more parameter, the Pride parameter (β). Some people include
 33 it in their models, but rarely. These phenomenological parameters are notoriously difficult
 34 to relate to the microstructure of real-life porous materials such as granular media, fibrous
 35 media or complicated foam structures. This fact makes the application of this kind of models
 36 for the inversion of microstructural properties of porous media from acoustical data rather
 37 difficult to understand by non-acousticians, e.g. by material scientists, process or chemical
 38 engineers.

39 It has recently been shown that the popular 6-parameter model¹ can be reduced to a
 40 4-parameter model because the two characteristic lengths and two permeabilities can be
 41 expressed via the median pore size (\bar{s}) and standard deviation in the pore size (σ_s) provided
 42 that the size of pores in the porous medium is log-normally distributed⁴, i.e.:

$$\Lambda = \bar{s} e^{-5/2(\sigma_s \log 2)^2}, \quad (1)$$

43

$$\Lambda' = \bar{s} e^{3/2(\sigma_s \log 2)^2}, \quad (2)$$

44

$$\kappa_0 = \frac{\bar{s}^2 \phi}{8\alpha_\infty} e^{-6(\sigma_s \log 2)^2}, \quad (3)$$

45 and

$$\kappa'_0 = \frac{\bar{s}^2 \phi}{8\alpha_\infty} e^{6(\sigma_s \log 2)^2}. \quad (4)$$

46 It has also been shown in⁴ that the Pride parameter³ for this type of porous media is:

$$\beta = 4/3 e^{4(\sigma_s \log 2)^2}. \quad (5)$$

47 A theoretical model which has a reduced number of parameters can be attractive to scientists
 48 and engineers who work beyond acoustics because: (i) the number of parameters in the
 49 model is greatly reduced; (ii) the porosity, median pore size and standard deviation in
 50 pore size become directly measurable; (iii) the physical meaning of the median pore size

51 and standard deviation in the pore size is easier to understand than the two characteristic
 52 lengths and thermal permeability. Effectively, the model by Horoshenkov *et al*⁴ suggests
 53 that the acoustical properties of a porous medium with log-normal pore size distribution
 54 can be predicted from the knowledge of ϕ , α_∞ , \bar{s} and σ_s . This reduction in the number
 55 of parameters in a model also paves the way for an easier inversion of key morphological
 56 characteristics of porous media from acoustical data which are relatively easy to obtain
 57 through a standard impedance tube experiment⁵.

58 However, one question which has been overlooked by the authors of⁴ is the relation
 59 between the tortuosity and the pore size distribution. Is the tortuosity of this kind of
 60 media a parameter independent from the pore size distribution statistics? This paper is an
 61 attempt to answer that question. It shows that the tortuosity of a porous medium with
 62 log-normally distributed pore size is controlled by the standard deviation in the pore size
 63 distribution. It is also shown how the acoustical impedance of a range of porous media
 64 (granular, fibrous and foams) can be predicted very accurately through the knowledge of
 65 the porosity and pore size distribution parameters only. The novelty of this paper is that
 66 it proposes a robust analytical model for the acoustical properties which relies on three
 67 directly measurable parameters of porous media. It also shows that the use of more than
 68 three parameters in the Johnson-Champoux-Allard-Lafarge model² is not necessary for many
 69 types of porous media. The significance of this paper is that it proposes an unambiguous
 70 relationship between the pore microstructure and key acoustical properties of porous media
 71 with log-normal pore size distribution. This new model is well suited for using acoustical
 72 data for measuring key non-acoustical properties of a wider range of porous media.

73 The paper is organised in the following manner. Section II proposes the new relation
 74 between the tortuosity and standard deviation in the pore size. Section III presents a
 75 revision of the model proposed in⁴. Section IV presents a comparison between the predicted
 76 and measured acoustical and non-acoustical properties of several types of porous media.
 77 Section V is the conclusions section.

78 II. THE TORTUOSITY OF POROUS MEDIA WITH LOG-NORMAL PORE SIZE 79 DISTRIBUTION

80 Let us assume that a sound wave propagates in a non-uniform pore which circular cross-
 81 section varies with depth as shown in Figure 1. In this figure Δx is the thickness of the

82 porous layer, Δl is the length of the section within which the change in the pore cross-section
 83 (A_n) is considered negligible. According to the work by Champoux and Stinson (see Eq.
 84 (20) in⁶) the electrically measured tortuosity of a medium with the total surface area (A)
 85 covered by M non-uniform pores is:

$$\alpha_\infty = \frac{\phi A}{M \Delta x} \sum_{n=1}^N \frac{\Delta l}{A_n}, \quad (6)$$

86 where N is the total number of cross-sectional changes which may occur in the pore area
 87 measured along the thickness of the porous layer, Δx (for more details see Figure 1 in ref.⁶).
 88 Since $\phi = \frac{M}{A \Delta x} \sum_n A_n \Delta l$, and $\Delta x = \sum_n \Delta l$ for a constant value of Δl equation (6) becomes:
 89

$$\alpha_\infty = \frac{\sum_{n=1}^N A_n \Delta l}{\left(\sum_{n=1}^N \Delta l \right)^2} \sum_{n=1}^N \frac{\Delta l}{A_n}. \quad (7)$$

90 Setting the total number of sections with a constant cross-section required to represent the
 91 complexity of the non-uniform pore shown in Figure 1 to $N \rightarrow \infty$, $\Delta l \rightarrow 0$ and swapping
 92 the sums in (7) for integrals yields (see eqs. (38)-(44) and eqs. (50), (51) in ref.⁴):

$$\alpha_\infty = \frac{I_A}{I_0^2} I_{1/A}, \quad (8)$$

93 where $I_A = \int_{-\infty}^{\infty} s^2 e(s) ds$, $I_{1/A} = \int_{-\infty}^{\infty} s^{-2} e(s) ds$ and $I_0 = \int_{-\infty}^{\infty} e(s) ds$ and $e(s)$ is the proba-
 94 bility density function for the pore radius s .

95 It is common in the areas of geotechnics and granular porous media research to use a
 96 logarithm with base 2 to express pore size on a log-normal scale, i.e. so that $s = 2^{-\varphi}$,
 97 $e(s) = f(\varphi) \frac{d\varphi}{ds}$, $f(\varphi) = \frac{1}{\sigma_s \sqrt{2\pi}} e^{-\frac{(\varphi - \bar{\varphi})^2}{2\sigma_s^2}}$ and $\varphi = -\log_2 s$. For this choice of pore size
 98 distribution it is possible to demonstrate that the above three integrals reduce to:

$$I_{1/A} = \int_{-\infty}^{+\infty} 2^{2\varphi} e^{-\frac{(\varphi - \bar{\varphi})^2}{2\sigma_s^2}} d\varphi = 2^{2\bar{\varphi}} e^{2\sigma_s^2 \log^2 2}, \quad (9)$$

$$I_A = \int_{-\infty}^{+\infty} 2^{-2\varphi} e^{-\frac{(\varphi - \bar{\varphi})^2}{2\sigma_s^2}} d\varphi = 2^{-2\bar{\varphi}} e^{2\sigma_s^2 \log^2 2}. \quad (10)$$

100 and

$$I_0 = \int_{-\infty}^{+\infty} e^{-\frac{(\varphi - \bar{\varphi})^2}{2\sigma_s^2}} d\varphi = 1. \quad (11)$$

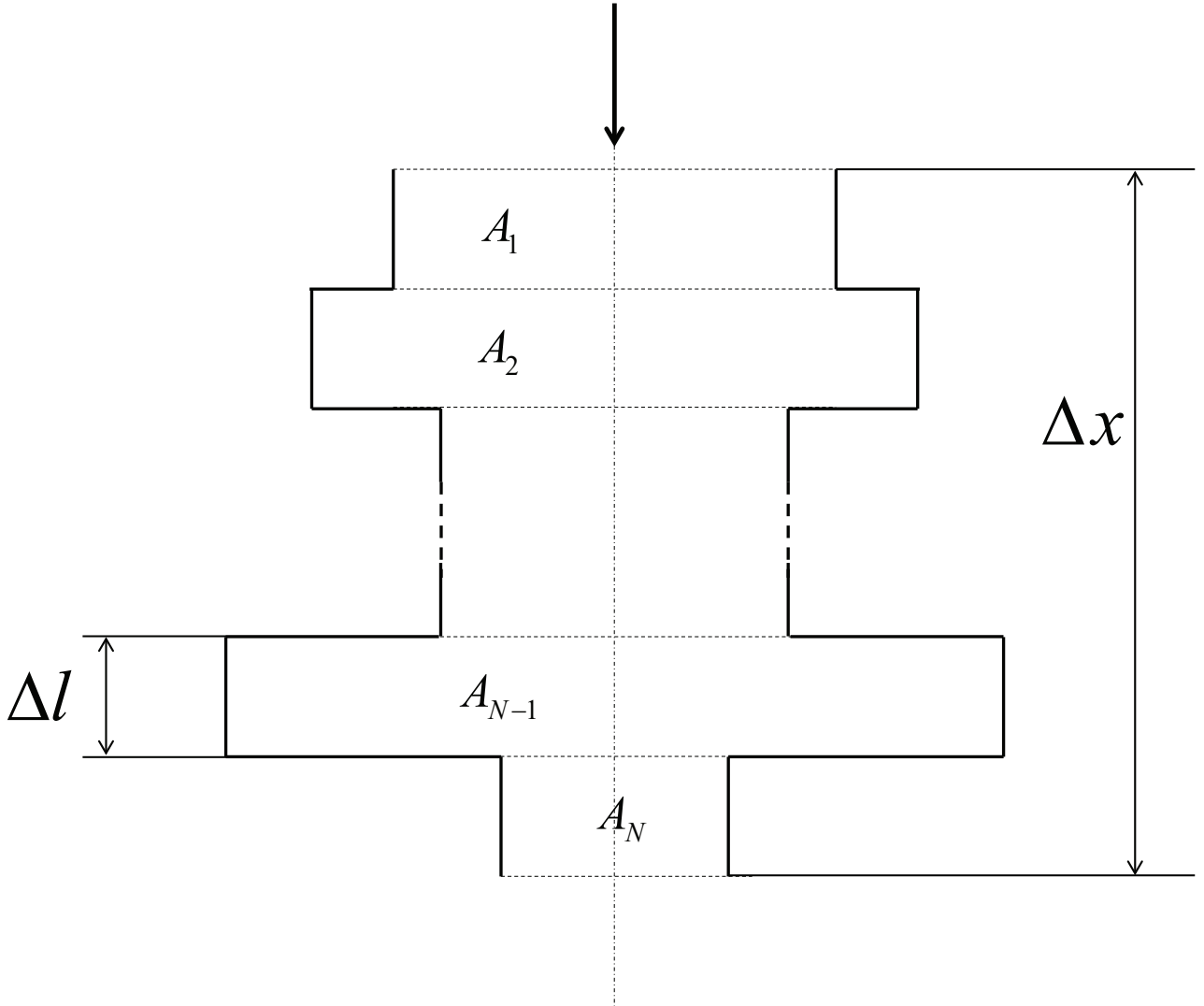


FIG. 1. Sound propagation in a non-uniform pore with a circular cross-section.

101 In these expressions $\bar{\varphi} = -\log_2 \bar{s}$ is the mean pore size on the logarithmic scale and \bar{s} is the
 102 median pore size on the linear pore size scale. The substitution of Eqs. (9)-(11) in Eq. (7)
 103 yields the new equation for the tortuosity:

$$\alpha_\infty = e^{4(\sigma_s \log 2)^2}. \quad (12)$$

104 Eq. (12) suggests that the tortuosity of a porous medium with well-interconnected non-
 105 uniform pores which size is log-normally distributed depends only on the standard deviation
 106 in the pore size (σ_s). In the limit case, when the pores are uniform and their size is identical,
 107 $\sigma_s = 0$ and $\alpha_\infty = 1$, which makes physical sense for materials with a relatively high porosity.

108 The main implication of Eq. (12) and previously derived expressions for the characteristic
 109 lengths and permeabilities (Eqs. (1)-(4)) is that it enables us to predict the acoustical
 110 properties of porous medium with three directly measurable parameters only rather than
 111 six^{1,2}. These parameters are: (i) the porosity (ϕ); (ii) the median pore size (\bar{s}); and (iii) the
 112 standard deviation in pore size distribution (σ_s).

113 III. MODELLING THE ACOUSTICAL PROPERTIES OF POROUS MEDIA 114 WITH THE 3-PARAMETER MODEL

115 Following⁴ we will propose Padé approximations for the equations for the frequency
 116 dependent bulk dynamic density ($\tilde{\rho}(\omega)$) and bulk complex compressibility ($\tilde{C}(\omega)$) in the
 117 equivalent fluid model to predict the acoustical properties of porous media with log normal
 118 distribution. Here ω stands for the circular frequency.

119 The bulk dynamic density can be approximated with the following expression (Eqs. (64)
 120 and (65) in⁴):

$$\tilde{\rho}(\omega)/\rho_0 \simeq \frac{\alpha_\infty}{\phi} \left(1 + \epsilon_\rho^{-2} \tilde{F}_\rho(\epsilon_\rho) \right), \quad (13)$$

121 where

$$\tilde{F}_\rho(\omega) = \frac{1 + \theta_{\rho,3}\epsilon_\rho + \theta_{\rho,1}\epsilon_\rho}{1 + \theta_{\rho,3}\epsilon_\rho} \quad (14)$$

122 is the Padé approximant to the viscosity correction function with $\epsilon_\rho = \sqrt{\frac{-i\omega\rho_0\alpha_\infty}{\phi\sigma}}$ (we
 123 note, there is a typo in the expression for ϵ_ρ in ref.⁴. The flow resistivity for a single pore
 124 (σ_x) must appear in the denominator. Also, the term (ρ_0) is missing from the denominator
 125 in the left hand side of Eq. (64) in⁴), $\theta_{\rho,1} = 1/3$, $\theta_{\rho,2} = e^{-1/2(\sigma_s \log 2)^2}/\sqrt{2}$ and $\theta_{\rho,3} = \theta_{\rho,1}/\theta_{\rho,2}$
 126 (see Section III in⁴). In these equations the bulk flow resistivity of the porous medium is
 127 (see also Eq. (3)):

$$\sigma = \frac{\eta}{\kappa_0} = \frac{8\eta\alpha_\infty}{\bar{s}^2\phi} e^{6(\sigma_s \log 2)^2}, \quad (15)$$

128 where η is the dynamic viscosity of air and ρ_0 is the ambient density of air.

129 Similarly, the bulk complex compressibility of the fluid in the material pores can be given
 130 in the following form (see Eqs. (68) and (69) in⁴):

$$\tilde{C}(\omega) = \frac{\phi}{\gamma P_0} \left(\gamma - \frac{\gamma - 1}{1 + \epsilon_c^{-2} \tilde{F}_c(\epsilon_c)} \right), \quad (16)$$

131 where

$$\tilde{F}_c(\epsilon_c) = \frac{1 + \theta_{c,3}\epsilon_c + \theta_{c,1}\epsilon_c}{1 + \theta_{c,3}\epsilon_c}. \quad (17)$$

132 In the above two equations $\epsilon_c = \sqrt{\frac{-i\omega\rho_0 N_{Pr}\alpha_\infty}{\phi\sigma'}}$, $\theta_{c,1} = \theta_{\rho,1} = 1/3$, $\theta_{c,2} = e^{3/2(\sigma_s \log 2)^2}$,
 133 $\theta_{c,3} = \theta_{c,1}/\theta_{c,2}$, γ is the ratio of specific heats, N_{Pr} is the Prandtl number and P_0 is the
 134 ambient atmospheric pressure. The thermal flow resistivity here is defined as as the inverse
 135 of the thermal permeability (see also Eq. (4)):

$$\sigma' = \frac{\eta}{\kappa'_0} = \frac{8\eta\alpha_\infty}{\bar{s}^2\phi} e^{-6(\sigma_s \log 2)^2}. \quad (18)$$

136 Eqs. (13) and (16) can be used to predict the characteristic acoustic impedance:

$$z_b(\omega) = \sqrt{\tilde{\rho}(\omega)/\tilde{C}(\omega)} \quad (19)$$

137 and complex wavenumber:

$$k_b(\omega) = \omega\sqrt{\tilde{\rho}(\omega)\tilde{C}(\omega)} \quad (20)$$

138 in a porous medium with log-normal pore size distribution.

139 IV. RESULTS

140 Eqs. (19) and (20) were used to predict the acoustical surface impedance of hard-backed
 141 layers of three types of porous media: (i) loose granular media; (ii) fibrous media; and (iii)
 142 foams. The details of these three types of media are given in Table I. The values of the
 143 intrinsic air properties (e.g. ρ_0 , η , γ and N_{Pr}) were calculated from the standard equations
 144 for the temperature of 20°C and ambient air pressure of $P_0 = 101320$ Pa. The equations
 145 for these parameters come from several textbooks. These equations were carefully compiled
 146 and provided kindly by Matelys⁸.

147 We chose glass beads because it has been shown that the pore size distribution in glass
 148 beads is very close to log-normal⁷. We chose melamine foam and rebound felt as the other
 149 two examples because these materials are commonly used as acoustic absorbers in various
 150 noise control applications.

151 The normalised surface impedance of finite, hard-backed layers of these porous media
 152 was calculated by:

$$z_s(\omega) = z_b(\omega) \coth(-ik_b(\omega)h)/(\rho_0 c_0), \quad (21)$$

153 where h is the layer thickness and c_0 is the sound speed in air. The measurements of the
 154 surface impedance of glass beads were carried out in a 45 mm diameter impedance tube.
 155 The measurements of the melamine foam and felt samples were made in a 100 mm diameter
 156 impedance tube. The both tubes were supplied by Materiacustica⁹. Each material sample
 157 was measured three times and the averaged data were used for the comparison with the
 158 model. The repeatability of the measurements was within $\pm 5\%$.

159 Figure 2 presents a comparison between the measured (dotted lines) and predicted (solid
 160 and dashed lines) normalized surface impedance of a 40 mm thick, hard-backed stack of 2
 161 mm diameter glass beads. These beads were deposited in the sample holder in a random
 162 manner and were left uncompacted. The solid lines correspond to the prediction made
 163 with the proposed Padé approximation model (equations (13) and (16)). The dashed lines
 164 correspond to the prediction made with the Johnson-Allard-Champoux-Lafarge model^{1,2}.
 165 The predictions correspond to the following values of the key non-acoustical parameters:
 166 $\phi = 0.376$, $\bar{s} = 305 \mu\text{m}$; and $\sigma_s = 0.388$. These non-acoustical parameters were estimated
 167 by fitting the Padé approximation model (Eqs. (13) and (16)) to the measured data for the
 168 surface impedance through the Nelder-Mead function minimization technique¹⁰ as described
 169 in¹¹. In this process the tortuosity and flow resistivity required for the Padé approximation
 170 model were predicted using Eqs. (12) and (3), respectively. The thermal permeability and
 171 characteristic lengths required for the subsequent comparison with the Johnson-Champoux-
 172 Allard model were predicted using Eqs. (1), (2) and (4), respectively. The values of all these
 173 parameters for glass beads and for other materials studied in this work are summarized in
 174 Table I.

175 The results obtained for glass beads suggest that the viscous characteristic length we
 176 recovered from the acoustical data is consistent with that reported by Glover *et al* for 2
 177 mm glass beads¹² (this work: $\Lambda = 255 \mu\text{m}$; Table 1 in Glover *et al*¹²: $\Lambda = 252 \mu\text{m}$). The
 178 compaction states for these two materials were comparable so that the porosities were similar
 179 (in this work: $\phi = 0.376$; Glover *et al*¹²: $\phi = 0.386$). The porosity value estimated from
 180 our experiment is also consistent with that measured by Leclaire *et al* for uncompacted
 181 glass beads. It was shown to be in the range of $0.362 \leq \phi \leq 0.385$ (see Table I in⁷). The
 182 estimated value of the median pore size for our glass beads seems sensible because the work
 183 by Glover *et al* (page E20 in¹²) suggests that the ratio of the sphere diameter (2 mm) to
 184 the effective pore diameter ($611 \mu\text{m}$) in a stack of identical beads should be 3.44, which
 185 makes our estimate of \bar{s} accurate within 5%. Our estimate of the thermal characteristic

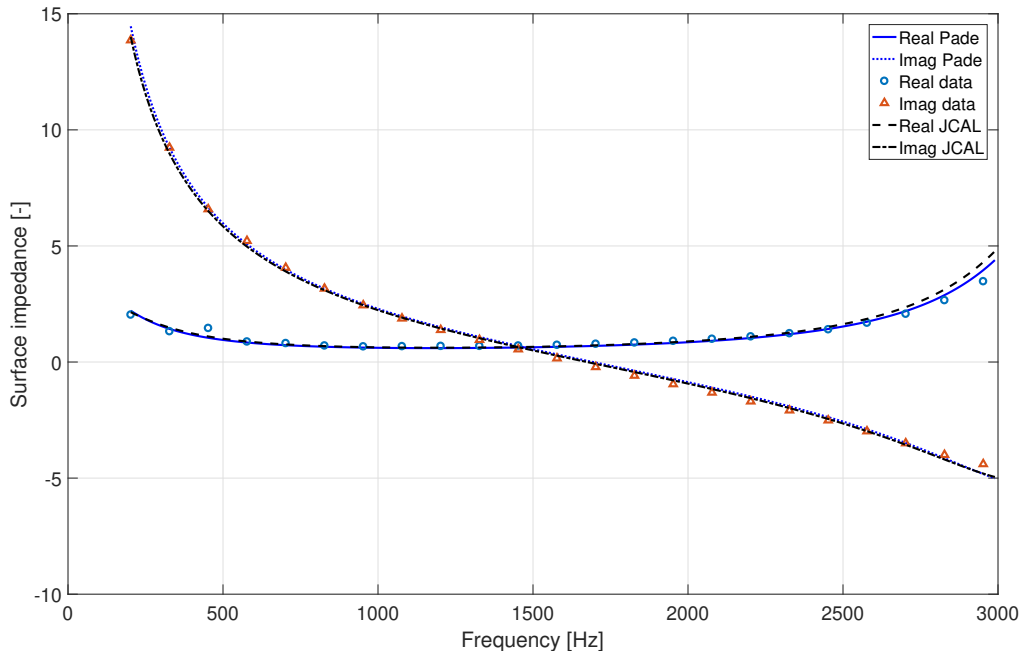


FIG. 2. The measured and predicted normalized surface impedance of a 40 mm thick, hard-backed layer of 2mm diameter glass beads.

186 length ($\Lambda' = 340 \mu\text{m}$) also makes sense because it scales favourably to $\Lambda' = 321 \mu\text{m}$ from
187 $\Lambda' = 263 \mu\text{m}$ measured by Leclaire *et al* for 1.64 mm diameter glass beads in an independent
188 water suction experiment (see Table II in⁷).

189 On the other hand, the flow resistivity predicted with Eqs. (3 and (15)) ($\sigma = 8560 \text{ Pa s}$
190 m^{-2}) was found to be 17% higher than that we measured at the University of Sheffield with
191 an AFD AcoustiFlow 300 device on 100 mm diameter samples. This apparatus was supplied
192 by Akustik Forschung Dresden and used alongside their AFD 311 software package¹³. This
193 discrepancy can be related to differences in the packing conditions and diameters of the
194 sample holders used in the impedance tube and flow resistivity experiments. The estimated
195 value of tortuosity for our glass beads ($\alpha_\infty = 1.33$) is consistent with that one can estimate
196 from a typical value of the formation factor

$$F \approx \alpha_\infty / \phi, \quad (22)$$

197 which, according to literature (e.g.^{12,14}), can be in the range of $3.0 \leq F \leq 4.0$ for a stack of
198 uniform spherical beads. This suggests that the tortuosity of our glass beads should be in
199 the range of $1.13 \leq \alpha_\infty \leq 1.50$. Our tortuosity estimate of $\alpha_\infty = 1.33$ is very close to the
200 median for this range.

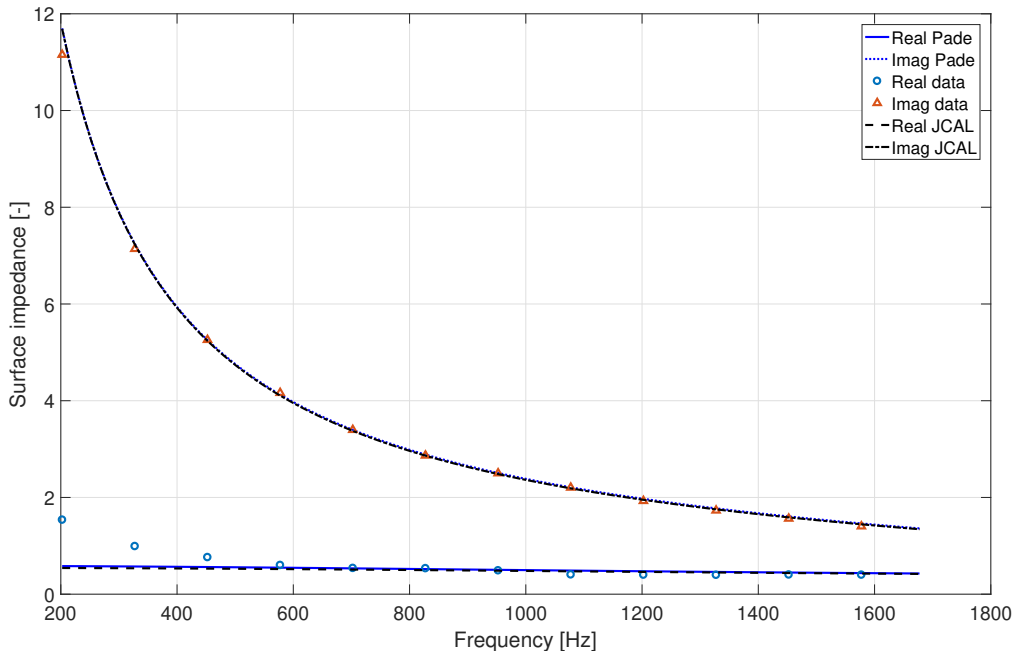


FIG. 3. The measured and predicted normalized surface impedance of a 16.5 mm thick, hard-backed layer of melamine foam used in a range of acoustic applications.

201 The results presented in Figure 2 show that the Padé approximation model used with a set
202 of sensible values of the three key non-acoustic parameters predicts the real and imaginary
203 part of the impedance with the normalized mean error of $\pm 4.4\%$. This error was calculated
204 as:

$$E = \frac{\sum \|z_s^{(m)} - z_s^{(p)}\|}{\|z_s^{(m)}\|}, \quad (23)$$

205 where the indices (m) and (p) stand for the measured and predicted values, respectively.

206 For this set of parameters the Johnson-Champoux-Allard model predicts the impedance
207 with the normalized mean error of $\pm 4.0\%$. These errors are within the experimental accuracy
208 of the impedance tube apparatus used in this work.

209 Figure 3 presents the normalized surface impedance of a 16.5 mm thick, hard-backed
210 layer of melamine foam. Similarly to the results presented in Figure 2 the parameters of the
211 best fit were obtained through the minimization procedure described in¹¹. The parameters
212 of best fit are: $\phi = 0.998$, $\bar{s} = 115 \mu\text{m}$; and $\sigma_s = 0.243$. These and other parameters for this
213 material are listed in Table I. The predictions by the two models made for this material are
214 almost identical. The normalized mean error between the two models and measured data is
215 within $\pm 2.4\%$. The two models are not very sensitive to the value of the porosity because

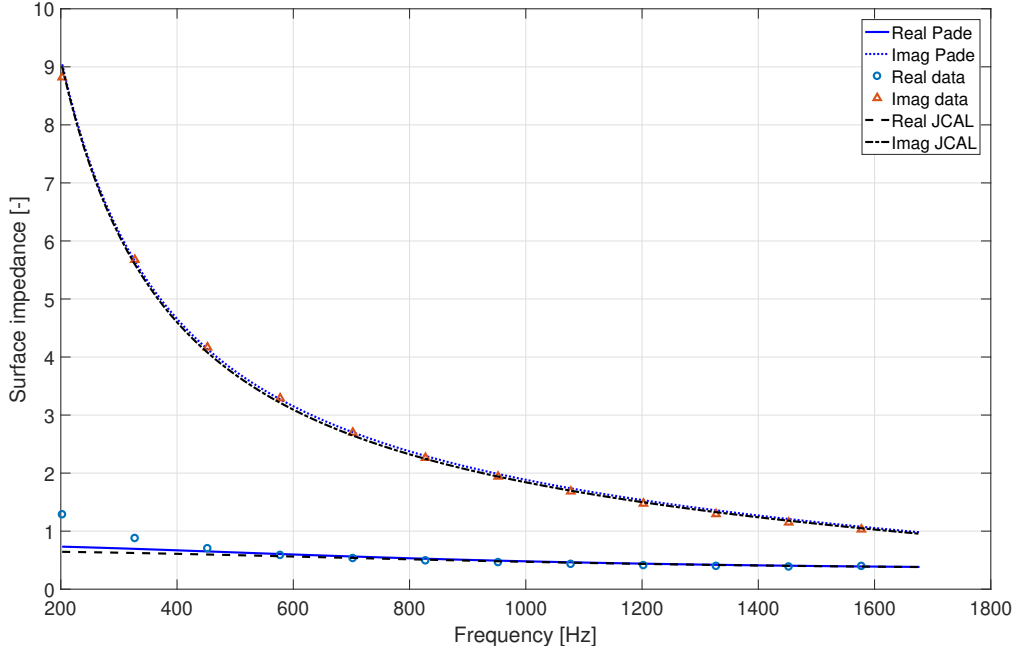


FIG. 4. The measured and predicted normalized surface impedance of a 21.5 mm thick, hard-backed layer of rebound felt used in automotive noise control applications.

216 its true value is close to unity ($\phi = 99.3\%$). The estimated median pore size ($\bar{s} = 115 \mu\text{m}$)
 217 makes sense because typical pore count in melamine foams is 150-200 cells per inch¹⁵, which
 218 suggests that the average cell size should be in the range of 127 – 169 μm . For similar
 219 melamine foam (see page 94 in¹⁶) it was estimated from optical images at $\bar{s} = 128 \pm 67 \mu\text{m}$,
 220 which makes our estimate fall within the experimental error. Our estimate for the flow
 221 resistivity of melamine foam (Eqs. (3) and (15)) is $\sigma = 14600 \text{ Pa s m}^{-2}$. This is 10.4%
 222 below the value of $\sigma = 16400 \text{ Pa s m}^{-2}$ measured with our flow resistivity apparatus¹³. The
 223 standard deviation in the pore size in this material is relatively small ($\sigma_s = 0.243$). As a
 224 result, the tortuosity estimated with Eq. (12) is close to unity ($\alpha_\infty = 1.12$) and it is not a
 225 dominant parameter in this case.

226 Finally, Figure 4 presents the normalized surface impedance for a 21.5 mm layer of re-
 227 bound felt used as an acoustic lining in vehicles. Here we compare the predictions with the
 228 two models against measured data. This material corresponds to Sample 3 described and
 229 characterized in detail in¹⁷. The parameters of best fit for this material are: $\phi = 0.998$,
 230 $\bar{s} = 147 \mu\text{m}$; and $\sigma_s = 0.325$. These and other parameters for this material are listed in
 231 Table I. The estimated value of porosity is 3% higher than the $\phi = 0.97$ value reported in¹⁷.
 232 It is easy to check that this small discrepancy has only a marginal effect on the predicted

TABLE I. The values of non-acoustical parameters for the three materials studied in this work. The values in brackets correspond to those which were measured directly and non-acoustically.

Material	h,	\bar{s} ,	ϕ	σ_s ,	σ ,	κ'_0 ,	Λ ,	Λ' ,
	mm	μm		φ -units	Pa s m^{-2}	m^2	μm	μm
2 mm glass beads	(40.0)	305	0.376	0.388	8560	5.06×10^{-9}	255	340
					(7290)		(253)	(321)
melamine foam	(16.5)	115	0.998	0.243	14600	1.75×10^{-9}	107	120
			(0.993)		(16400)			
rebound felt	(21.5)	147	0.998	0.325	11000	2.99×10^{-9}	131	160
			(0.970)		(10260)			

233 impedance because the acoustical behaviour of this material is dominated by the pore size
234 and it is relatively insensitive to small variations in the porosity value. The normalized
235 mean error between the measured data and prediction with the Padé approximation model
236 is $\pm 1.5\%$. The normalized mean error between the measured data and prediction with the
237 Johnson-Champoux-Allard model is $\pm 1.8\%$. There is a small difference between the pre-
238 dictions made with the Johnson-Champoux-Allard model and Padé approximation. This
239 difference can be reduced by adjusting the porosity between the measured ($\phi = 0.97$) and
240 estimated ($\phi = 0.998$) values. The flow resistivity of this material estimated using Eqs. (3)
241 and (15) is $\sigma = 11000 \text{ Pa s m}^{-2}$. This value compares very well against the measured flow
242 resistivity of $\sigma = 10260 \pm 180 \text{ Pa s m}^{-2}$ and it is within the experimental error. The stan-
243 dard deviation in the pore size in this material ($\sigma_s = 0.325$) is higher than that estimated
244 for melamine foam ($\sigma_s = 0.243$). As a result, the tortuosity estimated with Eq. (12) is
245 noticeably higher than unity ($\alpha_\infty = 1.22$) and it is becoming an influential parameter in the
246 modelling process.

247 V. CONCLUSIONS

248 This paper proposes a new equation for the tortuosity of porous media with pore size close
249 to log-normal (Eq. (12)) suggesting that the tortuosity of this kind of media is dependent

250 on the standard deviation in the pore size only. This new equation can be combined with
 251 equations (1) - (4) to effectively halve the number of non-acoustical parameters used in
 252 the popular Johnson-Champoux-Allard model^{1,2}. It has been demonstrated through an
 253 experiment that this model can be used to predict accurately the acoustical properties of
 254 granular media, fibrous media and foams with three non-acoustical parameters only. These
 255 parameters are: (i) median pore size (\bar{s}); (ii) porosity (ϕ); and (iii) standard deviation in
 256 the log-normal pore size distribution (σ_s).

257 The paper also proposes a new Padé approximation model for the prediction of the
 258 acoustical properties of porous media with non-uniform pore size and pore size distribution
 259 close to log-normal. This model can be used as an alternative to the Johnson-Champoux-
 260 Allard model. It has been shown that the predictions with these two models are almost
 261 identical and close to our measured surface impedance data within $\pm 4\%$.

262 An approach to reduce the number of non-acoustical parameters in an acoustical model
 263 seems very useful because it enables us to make an accurate estimation of key parameters
 264 of pore size distribution and porosity in various types of porous media from acoustical data.
 265 It also enables us to relate these quantities to those parameters in the Johnson-Champoux-
 266 Allard model which are difficult or impossible to measure non-acoustically. This makes
 267 application of this approach more attractive for the inversion of microstructural properties of
 268 porous media from acoustical data by non-acousticians, e.g. by material scientists, chemical,
 269 process or geotechnical engineers.

270 ACKNOWLEDGMENTS

271 This research has been partially supported by the EU COST Denorms (CA15125), EP-
 272 SRC UK Acoustics Network (EP/R005001) and EPSRC-sponsored Centre for Doctoral
 273 Training in Polymers, Soft Matter and Colloids at Sheffield. We are also grateful to Dr.
 274 Andre Revil, Université Savoie Mont-Blanc (France), for suggesting to include some rele-
 275 vant references to granular media research.

276 REFERENCES

277 ¹Y. Champoux and J. F. Allard, Dynamic tortuosity and bulk modulus in air-saturated
 278 porous media, *J. Appl. Phys.*, **70**(4), 1975-1979 (1991).

- 279 ²D. Lafarge, P. Lemarinier, J.-F. Allard, V. and Tarnow, Dynamic compressibility of air in
280 porous structures at audible frequencies, *J. Acoust. Soc. Am.* **102**(4), 1995-2006 (1997).
- 281 ³S. R. Pride, F. D. Morgan and A. F. Gangi, Drag forces in porous medium acoustics, *J.*
282 *Phys. Rev. B* **47**, 4964-4978 (1993).
- 283 ⁴K. V. Horoshenkov, J.-P. Groby and O. Dazel, Asymptotic limits of some models for
284 sound propagation in porous media and the assignment of the pore characteristic lengths,
285 *J. Acoust. Soc. Am.*, **139**(5), 2463-2474 (2016).
- 286 ⁵ISO 10534-2:1998, Determination of sound absorption coefficient and impedance in
287 impedance tubes, Part 2: Transfer-function method, International Organization for Stan-
288 dardization, Geneva, Switzerland, (1998).
- 289 ⁶Y. Champoux and M. R. Stinson, On acoustical models for sound propagation in porous
290 materials and the influence of shape factors, *J. Acoust. Soc. Am.*, **92**(2), 1120 – 1131,
291 (1992).
- 292 ⁷P. Leclaire, M. J. Swift, and K. V. Horoshenkov, Determining the specific area of porous
293 acoustic materials from water extraction data, *J. Appl. Phys.*, 84 (12), 6886 – 6890 (1998).
- 294 ⁸<http://http://apmr.matelys.com/>. Last accessed on 19 March 2019.
- 295 ⁹http://www.materiacustica.it/mat_UKProdotti_3Mics.html. Last accessed on 27 De-
296 cember 2018.
- 297 ¹⁰J. A. Nelder and R. Mead, A simplex method for function minimization, *Comput. J.* **7**,
298 308313 (1965).
- 299 ¹¹K. V. Horoshenkov, A. Khan, and H. Benkreira, Acoustic properties of low growing plants,
300 *J. Acoust. Soc. Am.* **133** (5), 25542565 (2013)
- 301 ¹²P. W. J. Glover and E. Walker, Grain-size to effective pore-size transformation derived
302 from electrokinetic theory, *Geophysics* **74** (1), E17E29 (2009).
- 303 ¹³[https://www.akustikforschung.de/en/produkte/messgerate/
304 stromungswiderstandsmessgerat-aed-300-acoustiflow/](https://www.akustikforschung.de/en/produkte/messgerate/stromungswiderstandsmessgerat-aed-300-acoustiflow/). Last accessed on 27
305 December 2018.
- 306 ¹⁴Q. Niu, A. Revil, Z. Li and Y.-H. Wang, Relationship between electrical conductivity
307 anisotropy and fabric anisotropy in granular materials during drained triaxial compressive
308 tests: a numerical approach, *Geophys. J. Int.* **210**, 117 (2017).

309 ¹⁵http://www.soundservice.co.uk/melamine_foam_tech_spec.html. Last accessed on
310 27 December 2018.

311 ¹⁶K. V. Horoshenkov, A review of acoustical methods for porous material characterisation,
312 *Int. J. Acoust. Vib.*, **22**(1), 92-103 (2016).

313 ¹⁷A. I. Hurrell, K. V. Horoshenkov, and M. T. Pelegrinis, The accuracy of some models for
314 the airflow resistivity of nonwoven materials, *J. Appl. Acoust.*, **130** 230-237 (2018).

315 **LIST OF FIGURES**

316 Figure 1: Sound propagation in a non-uniform pore with a circular cross-section.

317 Figure 2. The measured and predicted normalized surface impedance of a 40 mm thick,
318 hard-backed layer of 2 mm diameter glass beads.

319 Figure 3. The measured and predicted normalized surface impedance of a 16.5 mm thick,
320 hard-backed layer of melamine foam used in a range of acoustic applications.

321 Figure 4. The measured and predicted normalized surface impedance of a 21.5 mm thick,
322 hard-backed layer of rebound felt used in automotive noise control applications.